© 2019 IJSRSET | Volume 6 | Issue 1 | Print ISSN: 2395-1990 | Online ISSN : 2394-4099
Themed Section : Engineering and Technology
DOI : https://doi.org/10.32628/IJSRSET196164

Advance in Layered-Structures of Piezoelectricity

Yi Xiao
Research School of Engineering, Australian National University, Acton, ACT 2601, Australia

ABSTRACT

This paper presents an overview of layered structures of piezoelectric materials. Developments of layered structures in piezoelectric materials are presented. Finally, a brief summary of the approaches discussed is provided and future trends in this field are identified.

Keywords : Piezoelectric Materials, Penny-Shaped Crack, Piezoelectric Cylinder

I. INTRODUCTION

Piezoelectric material is such that when it is subjected to a mechanical load, it generates an electric charge. This effect is usually called the "piezoelectric effect". Conversely, when piezoelectric material is stressed electrically by a voltage, its dimension change. This phenomenon is known as the "inverse piezoelectric effect". The study of piezoelectricity was initiated by J. and P. Curie in 1880 [1]. They found that certain crystalline materials generate an electric charge proportional to a mechanical stress. Since then new theories and applications of the field have been constantly advanced [2-10]. Voigt [2] developed the first complete and rigorous formulation of piezoelectricity in 1890. Since then several books on the phenomenon and theory of piezoelectricity have been written. Among them are the references by Cady [3], Tiersten [4], Parton and Kudryavtsev [5], Ikeda [6], Rogacheva [7], Qin [8-11], and Qin and Yang [12]. The first of these [2] treated the physical properties of piezoelectric crystals as well as their practical applications, the second [3] dealt with the linear equations of vibrations in piezoelectric materials, and the third and fourth [4, 5] gave a more detailed description of the physical properties of piezoelectricity. Rogacheva [7] presented general theories of piezoelectric shells. Qin [8-11] discussed Green's functions, advanced theory, and fracture mechanics of piezoelectric materials as well as applications to bone remodelling. Micromechanics of the piezoelectricity were discussed in [12]. These advances have resulted in a great number of publications including journal and conference papers. These include but not limit to applications to Branched crack problems[13-15], experimental investigation of bone materials [16-21], multi-field problems of bone remodelling [22-29], decay analysis of dissimilar laminates [30], moving crack problems [31], anti-plane crack problems [32, 33], fibre-pull out [34], fibre-push out [35-37], problems of frog Sartorius muscles [38], effective property evaluation [39-42], Green's function analysis [43-50], derivation of general solutions [51-55], boundary element analysis [56-63], micro-macro crack interaction problems [64], Trefftz finite element analysis [65-70], crack-inclusion problems [71, 72], crack growth problem [73, 74], multi-crack problems [75], crack-interface problems [76-78], closed crack-tip analysis [79], crack-path selection [80], penny-shaped crack analysis [81, 82], logarithmic singularity analysis [83], multi-layer piezoelectric actuator [84, 85], Symplectic mechanics analysis [86], fibre-reinforced composites [87], interlayer stress analysis [88], coupled thermo-electro-chemo-mechanical analysis [89], and damage analysis [90, 91].

Based on the analysis above, the present review consists of two major sections. Problems of multilayer magneto-electro-elastic plates adhesively bonded by viscoelastic interlayer are discussed in Section 2. Section 3 focuses on solutions of layered magneto-electro-elastic cylindrical shell with viscoelastic interlayer. Finally, a brief summary on these sections is provided and areas that need further research are identified.

II. magneto-electro-elastic plates adhesively bonded by viscoelastic interlayer

All formulations in this section are taken from the work of Wu et al [92]. In their paper, they consider simply supported multilayer magneto-electro-elastic plate adhesively bonded by viscoelastic interlayer subjected to transverse loading. We discuss here analytical solutions, rather than numerical solutions of engineering problems [93-110]. As shown in Figure 1, we consider a layered plate of length a, width b and thickness H, consisting of p orthotropic magneto-electro-elastic layers of thickness h_i , which are adhesively bonded by p-1 viscoelastic interlayers, each of thickness Δh. The plate is simply supported at four sides and loaded by distributed mechanical loading q(x,y) acting over the top surface. A Cartesian coordinate O-xyz is established with the origin O located at the corner of the bottom surface. d_i^0 and d_i^1 denote the distances from the lower and upper surfaces of the i-th layer to the bottom surface of the plate, respectively.

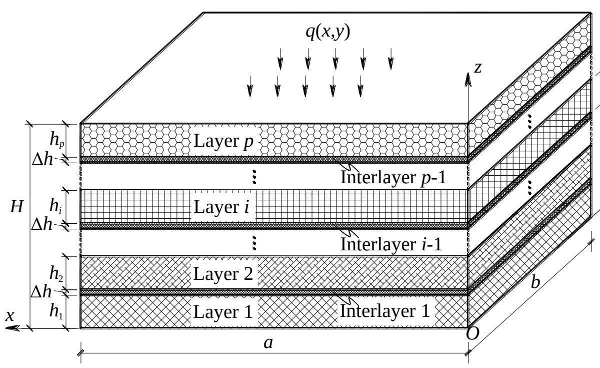

Figure 1. Multilayer magneto-electro-elastic plate with viscoelastic interlayer.

Basic equations of a magneto-electro-elastic layer

Based on the 3D equations of magneto-electro-elasticity, the coupled constitutive equations for i-th magneto-electro-elastic layer can be given in the form of tensor, as follows:

$$\sigma_j^i = c_{jk}^i \gamma_k^i - e_{kj}^i E_k^i - q_{kj}^i H_k^i \,,\ D_j^i = e_{jk}^i \gamma_k^i + \varepsilon_{jk}^i E_k^i + d_{jk}^i H_k^i \,,$$
$$B_j^i = q_{jk}^i \gamma_k^i + d_{jk}^i E_k^i + \mu_{jk}^i H_k^i \,,\ \text{i=1,2…p}, \tag{1}$$

where σ_j^i , γ_k^i , D_j^i , E_k^i , B_j^i and H_k^i stand for the stress, strain, electric displacement, electric field, magnetic induction and magnetic field, respectively; c_{jk}^i , e_{kj}^i , q_{kj}^i , ε_{jk}^i , d_{jk}^i and μ_{jk}^i are elastic, piezoelectric, piezo-magnetic, dielectric, magnetic-permeability and magneto-electric constants, respectively, which are detailly expressed in Eq. (A1) in Appendix A. The general strain-displacement relations are governed by

$$\gamma_{kj}^i = 0.5(u_{k,j}^i + u_{j,k}^i) \,,\ E_j^i = -\phi_{,j}^i \,,\ H_j^i = -\psi_{,j}^i \,,\ \text{i=1,2…p}, \tag{2}$$

where u_k^i , ϕ^i and ψ^i are elastic displacement, electric and magnetic potentials, respectively, and $[u^i] = [u_x^i \quad u_y^i \quad u_z^i]^T$. The equilibrium equations, in absence of body forces, electric charge and current density, are given by

$$\sigma_{kj,j}^i = 0 \,,\ D_{j,j}^i = 0 \,,\ B_{j,j}^i = 0 \,,\ \text{i=1,2…p}. \tag{3}$$

By using the state approach [111], the partial differential equations for the out-of-plane variables can be obtained from Eqs. (1)-(3), as follows

$$\frac{\partial}{\partial z}\mathbf{X}^i(x,y,z,t) = \mathbf{M}\mathbf{X}^i(x,y,z,t) \,,\ \text{i=1,2…p}, \tag{4}$$

where $\mathbf{M}$ is given in Eq. (A2) in Appendix A; $\mathbf{X}^i$ is the state vector including ten out-of-plane variables, i.e., $\mathbf{X}^i = [u_x^i \quad u_y^i \quad D_z^i \quad B_z^i \quad \sigma_z^i \quad \tau_{xz}^i \quad \tau_{yz}^i \quad \phi^i \quad \psi^i \quad u_z^i]^T$. The boundary conditions for the simply supported plate can be expressed by

$$\sigma_x^i = v^i = w^i = \phi^i = \psi^i = 0 \,,\ \text{at x=0, a}, \tag{5}$$
$$\sigma_y^i = u^i = w^i = \phi^i = \psi^i = 0 \,,\ \text{at y=0, b}.$$

For this boundary conditions, the ten out-of-plan variables in $\mathbf{X}^i$ can be expanded in the double Fourier series form:

$$\begin{bmatrix} u_x^i(x,y,z,t) \\ u_y^i(x,y,z,t) \\ D_z^i(x,y,z,t) \\ B_z^i(x,y,z,t) \\ \sigma_z^i(x,y,z,t) \\ \tau_{xz}^i(x,y,z,t) \\ \tau_{yz}^i(x,y,z,t) \\ \phi^i(x,y,z,t) \\ \psi^i(x,y,z,t) \\ u_z^i(x,y,z,t) \end{bmatrix} = \sum_{m=1}^{\infty}\sum_{n=1}^{\infty} \begin{bmatrix} u_{x,mn}^i(z,t)\cos(\alpha_m x)\sin(\beta_n y) \\ u_{y,mn}^i(z,t)\sin(\alpha_m x)\cos(\beta_n y) \\ D_{z,mn}^i(z,t)\sin(\alpha_m x)\sin(\beta_n y) \\ B_{z,mn}^i(z,t)\sin(\alpha_m x)\sin(\beta_n y) \\ \sigma_{z,mn}^i(z,t)\sin(\alpha_m x)\sin(\beta_n y) \\ \tau_{xz,mn}^i(z,t)\cos(\alpha_m x)\sin(\beta_n y) \\ \tau_{yz,mn}^i(z,t)\sin(\alpha_m x)\cos(\beta_n y) \\ \phi_{mn}^i(z,t)\sin(\alpha_m x)\sin(\beta_n y) \\ \psi_{mn}^i(z,t)\sin(\alpha_m x)\sin(\beta_n y) \\ u_{z,mn}^i(z,t)\sin(\alpha_m x)\sin(\beta_n y) \end{bmatrix},$$

i=1,2…p, (6)

where $\alpha_m = m\pi/a$ and $\beta_n = n\pi/b$. By substituting Eq. (6) into Eq. (4), one obtains

$$\frac{d}{dz}\mathbf{X}_{mn}^i(z,t) = \mathbf{K}_{mn}^i \mathbf{X}_{mn}^i(z,t), \text{ m,n=1,2,3…, i=1,2… p,} \quad (7)$$

where

$\mathbf{X}_{mn}^i = [u_{x,mn}^i \quad u_{y,mn}^i \quad D_{z,mn}^i \quad B_{z,mn}^i \quad \sigma_{z,mn}^i \quad \tau_{xz,mn}^i \quad \tau_{yz,mn}^i \quad \phi_{mn}^i \quad \psi_{mn}^i \quad u_{z,mn}^i]^T$; $\mathbf{K}_{mn}^i$ is defined in Eq. (A3) in Appendix A. The solution of Eq. (7) is $\mathbf{X}_{mn}^i(z,t) = e^{\mathbf{K}_{mn}^i z}\mathbf{C}_{mn}^i(t)$, m,n=1,2,3…, i=1,2… p, (8)

where $\mathbf{C}_{mn}^i(t) = [c_{1,mn}^i(t) \quad c_{2,mn}^i(t) \quad \cdots \quad c_{10,mn}^i(t)]^T$ is a vector involving undetermined time-varying coefficients. Let us define

$$\mathbf{\Psi}_{mn}^i(z) = e^{\mathbf{K}_{mn}^i z} = \begin{bmatrix} \mathbf{T}_{1,mn}^i(z) \\ \mathbf{T}_{2,mn}^i(z) \\ \cdots \\ \mathbf{T}_{10,mn}^i(z) \end{bmatrix} = \begin{bmatrix} T_{11,mn}^i(z) & T_{12,mn}^i(z) & \cdots & T_{1,10,mn}^i(z) \\ T_{21,mn}^i(z) & T_{22,mn}^i(z) & \cdots & T_{2,10,mn}^i(z) \\ \cdots & \cdots & \cdots & \cdots \\ T_{10,1,mn}^i(z) & T_{10,2,mn}^i(z) & \cdots & T_{10,10,mn}^i(z) \end{bmatrix},$$

m,n=1,2,3…, i=1,2…p. (9)

By employing Eqs. (1) and (2), other in-plane variables can be expressed by the out-of-plane variables

$$\sigma_x^i = \sum_{m=1}^{\infty}\sum_{n=1}^{\infty}\{-\alpha_m c_{11}^i u_{mn}^i - \beta_n c_{12}^i v_{mn}^i + [c_{13}^i \quad e_{31}^i \quad q_{31}^i](\boldsymbol{\kappa}^i)^{-1}\mathbf{w}_{mn}^i\}\sin(\alpha_m x)\sin(\beta_n y)$$

$$\sigma_y^i = \sum_{m=1}^{\infty}\sum_{n=1}^{\infty}\{-\alpha_m c_{12}^i u_{mn}^i - \beta_n c_{22}^i v_{mn}^i + [c_{23}^i \quad e_{32}^i \quad q_{32}^i](\boldsymbol{\kappa}^i)^{-1}\mathbf{w}_{mn}^i\}\sin(\alpha_m x)\sin(\beta_n y)$$

$$D_x^i = \sum_{m=1}^{\infty}\sum_{n=1}^{\infty}\{\frac{e_{15}^i}{c_{55}^i}\tau_{xz,mn}^i - \alpha_m[\varepsilon_{11}^i + \frac{(e_{15}^i)^2}{c_{55}^i}]\phi_{mn}^i - \alpha_m[d_{11}^i + \frac{e_{15}^i q_{15}^i}{c_{55}^i}]\psi_{mn}^i\}\cos(\alpha_m x)\sin(\beta_n y)$$

$$D_y^i = \sum_{m=1}^{\infty}\sum_{n=1}^{\infty}\{\frac{e_{24}^i}{c_{44}^i}\tau_{yz,mn}^i - \beta_n[\varepsilon_{22}^i + \frac{(e_{24}^i)^2}{c_{44}^i}]\phi_{mn}^i - \beta_n[d_{22}^i + \frac{e_{24}^i q_{24}^i}{c_{44}^i}]\psi_{mn}^i\}\sin(\alpha_m x)\cos(\beta_n y)$$

$$B_x^i = \sum_{m=1}^{\infty}\sum_{n=1}^{\infty}\{\frac{q_{15}^i}{c_{55}^i}\tau_{xz,mn}^i - \alpha_m[d_{11}^i + \frac{e_{15}^i q_{15}^i}{c_{55}^i}]\phi_{mn}^i - \alpha_m[\mu_{11}^i + \frac{(q_{15}^i)^2}{c_{55}^i}]\psi_{mn}^i\}\cos(\alpha_m x)\sin(\beta_n y),$$

$$B_y^i = \sum_{m=1}^{\infty}\sum_{n=1}^{\infty}\{\frac{q_{24}^i}{c_{44}^i}\tau_{yz,mn}^i - \beta_n[d_{22}^i + \frac{e_{24}^i q_{24}^i}{c_{44}^i}]\phi_{mn}^i - \beta_n[\mu_{22}^i + \frac{(q_{24}^i)^2}{c_{44}^i}]\psi_{mn}^i\}\sin(\alpha_m x)\cos(\beta_n y),$$

$$\tau_{xy}^i = \sum_{m=1}^{\infty}\sum_{n=1}^{\infty}[\beta_n c_{66}^i u_{mn}^i(z,t) + \alpha_m c_{66}^i v_{mn}^i(z,t)]\cos(\alpha_m x)\cos(\beta_n y),$$

i=1,2…p. (10)

where

$$\mathbf{w}_{mn}^i = \begin{bmatrix} \sigma_{z,mn}^i + \alpha_m c_{13}^i u_{mn}^i + \beta_n c_{23}^i v_{mn}^i \\ D_{z,mn}^i + \alpha_m e_{31}^i u_{mn}^i + \beta_n e_{32}^i v_{mn}^i \\ B_{z,mn}^i + \alpha_m q_{31}^i u_{mn}^i + \beta_n q_{32}^i v_{mn}^i \end{bmatrix}.$$

Basic equations of an adhesive interlayer

By the use of the standard linear solid model, the shear modulus of the adhesive interlayer is expressed as

$$G^*(t) = G_1^* e^{-t/\theta_G^*} + G_2^*, \quad (11)$$

where the superscript * means that the corresponding variable belongs to the interlayer, θ_G^* denotes the relaxation time ($\theta_G^* = \eta_G^*/G_1^*$), η_G^* the viscosity, G_1^* the relaxation moduli and G_2^* the long-term moduli. These parameters for viscoelastic materials can be tested by creep experiments [112]. The Poisson's ratio of the interlayer μ^* is assumed to be time-independent. Thus, the corresponding Young's modulus can be expressed by

$$E^*(t) = 2(1+\mu^*)G^*(t). \quad (12)$$

According to the theory for linear viscoelasticity [113], the constitutive equations in the interlayer are governed by

$$\sigma_z^{*i}(x,y,t) = E^*(t)\varepsilon_z^{*i}(x,y,0) + \int_0^t E^{*i}(t-\xi)\frac{\partial \varepsilon_z^{*i}(x,y,\xi)}{\partial \xi}d\xi,$$

$$\tau_{xz}^{*i}(x,y,t) = G^*(t)\gamma_{xz}^{*i}(x,y,0) + \int_0^t G^{*i}(t-\xi)\frac{\partial \gamma_{xz}^{*i}(x,y,\xi)}{\partial \xi}d\xi,$$

$$\tau_{yz}^{*i}(x,y,t) = G^*(t)\gamma_{yz}^{*i}(x,y,0) + \int_0^t G^{*i}(t-\xi)\frac{\partial \gamma_{yz}^{*i}(x,y,\xi)}{\partial \xi}d\xi,$$

i=1,2…p-1. (13)

These relations indicate the memory effect, i.e. the stress at a time is dependent on both current strain and strain history. For briefness, Eq. (13) is rewritten into the Stieltjes convolution form [114]

$$\sigma_z^{*i}(x,y,t) = \varepsilon_z^{*i}(x,y,t) \otimes dE^*(t),$$

$$\tau_{xz}^{*i}(x,y,t) = \gamma_{xz}^{*i}(x,y,t) \otimes dG^*(t),$$

$$\tau_{yz}^{*i}(x,y,t) = \gamma_{yz}^{*i}(x,y,t) \otimes dG^*(t), \text{ i=1,2…p-1,} \quad (14)$$

where the symbol ⊗ means the convolution operation. Recalling assumption (2), the strains in the interlayer can be further expressed as

$$\varepsilon_z^{*i}(x,y,t) = [u_z^{i+1}(x,y,d_{i+1}^0,t) - u_z^i(x,y,d_i^1,t)]/\Delta h,$$

$$\tau_{xz}^{*i}(x,y,t) = [u_x^{i+1}(x,y,d_{i+1}^0,t) - u_x^i(x,y,d_i^1,t)]/\Delta h,$$

$$\tau_{yz}^{*i}(x,y,t) = [u_y^{i+1}(x,y,d_{i+1}^0,t) - u_y^i(x,y,d_i^1,t)]/\Delta h,$$

i=1,2…p-1. (15)

The electric conditions between adjacent layers can be classified into three cases: (i) weakly dielectrically conducting condition; (ii) highly dielectrically conducting condition; (iii) the unelectroded condition [115]. For the first case, the normal electric displacement is continuous while the electric potential is discontinuous along the thickness direction. For the second case, the normal electric displacement and the electric potential are, respectively, discontinuous and continuous. The normal electric displacement and the electric potential in the third case are both continuous. The three electric conditions can be described as

$$D_z^{i+1}(x,y,d_{i+1}^0,t)-D_z^i(x,y,d_i^1,t)=\chi_1\left(\frac{\partial^2}{\partial x^2}+\frac{\partial^2}{\partial y^2}\right)\phi^i(x,y,d_i^1,t)\ ,$$

$$\phi^{i+1}(x,y,d_{i+1}^0,t)-\phi^i(x,y,d_i^1,t)=-\chi_2 D_z^i(x,y,d_i^1,t)\,,$$

i=1,2…p-1, (16)

in which, χ_1 =0 and χ_2 >0 represent the first condition, χ_1 >0 and χ_2 =0 represent the second and $\chi_1=\chi_2$ =0 is the last one.

The magnetic variables are assumed to be continuous along the adjacent layers, i.e.

$$B_z^{i+1}(x,y,d_{i+1}^0,t)=B_z^i(x,y,d_i^1,t)$$

$$\psi^{i+1}(x,y,d_{i+1}^0,t)=\psi^i(x,y,d_i^1,t)\ ,\ \text{i=1,2…p-1.} \tag{17}$$

Continuous and surface conditions

By combining Eqs. (6), (8), (9) and (14)-(17), the continuous conditions between the adjacent magneto-electro-elastic layers can be rearranged as

$$\mathbf{\Psi}_{mn}^{i+1}(d_{i+1}^0)\mathbf{C}_{mn}^{i+1}(t)-\mathbf{\Psi}_{mn}^i(d_i^1)\mathbf{C}_{mn}^i(t)=\mathbf{\Delta}_{mn}^i(t)\ ,\ \text{m,n=1,2,3…,}\ \text{i=1,2…p-1,} \tag{18}$$

where

$$\mathbf{\Delta}_{mn}^i(t)=[\delta_{i,mn}^{(u)}(t)\quad \delta_{i,mn}^{(v)}(t)\quad \delta_{i,mn}^{(D)}(t)\quad 0\quad 0\quad 0\quad 0\quad \delta_{i,mn}^{(\phi)}(t)\quad 0\quad \delta_{i,mn}^{(w)}(t)]^T$$

and

$$\tau_{xz,mn}^i(d_i^1,t)=\frac{\delta_{i,mn}^{(u)}(t)}{\Delta h}\otimes dG^*(t)\ ,$$

$$\tau_{yz,mn}^i(d_i^1,t)=\frac{\delta_{i,mn}^{(v)}(t)}{\Delta h}\otimes dG^*(t)\,,$$

$$\sigma_{z,mn}^i(d_i^1,t)=2(1+\mu^*)\frac{\delta_{i,mn}^{(w)}(t)}{\Delta h}\otimes dG^*(t)\ ,$$

$$D_{z,mn}^i(d_i^1,t)=-\frac{\delta_i^{(\phi)}(t)}{\chi_2}\,,$$

$$\left(\frac{\partial^2}{\partial x^2}+\frac{\partial^2}{\partial y^2}\right)\phi_{mn}^i(d_i^1,t)=\frac{\delta_{i,mn}^{(D)}(t)}{\chi_1}\ ,\ \text{m,n=1,2,3…, i=1,2…p-1.} \tag{19}$$

The boundary loadings, electric and magnetic conditions on the upper and lower surfaces are expressed

$$\sigma_z^1(x,y,0,t)=0\ ,\ \tau_{xz}^1(x,y,0,t)=0\ ,\ \tau_{yz}^1(x,y,0,t)=0\ ,$$
$$D_z^1(x,y,0,t)=0\ ,\ B_z^1(x,y,0,t)=0\ ,$$
$$\sigma_z^p(x,y,H,t)=-q(x,y)\ ,\ \tau_{xz}^p(x,y,H,t)=0\ ,$$
$$\tau_{yz}^p(x,y,H,t)=0\ ,\ D_z^p(x,y,H,t)=0\ ,\ B_z^p(x,y,H,t)=0\ , \tag{20}$$

where $q(x,y)$ can be expanded into double Fourier series, as follows

$$q(x,y)=\sum_{m=1}^{\infty}\sum_{n=1}^{\infty}q_{mn}\sin(\alpha_m x)\sin(\beta_n y)\ ,$$

$$q_{mn}=\frac{4}{ab}\int_0^a\int_0^b q(x,y)\sin(\alpha_m x)\sin(\beta_n y)\mathrm{d}x\mathrm{d}y\ . \tag{21}$$

By substituting Eqs. (6), (8) and (9) into Eq. (20) and then rearranging the results into matrix form, we have

$$\mathbf{M}_{mn}^1\mathbf{C}_{mn}^1(t)+\mathbf{M}_{mn}^p\mathbf{C}_{mn}^p(t)=\mathbf{Q}_{mn}\ ,\ \text{m,n=1,2,3…,} \tag{22}$$

where

$$\mathbf{M}_{mn}^1=[\mathbf{T}_{5,mn}^1(0)^T\quad \mathbf{T}_{6,mn}^1(0)^T\quad \mathbf{T}_{7,mn}^1(0)^T\quad \mathbf{T}_{3,mn}^1(0)^T\quad \mathbf{T}_{4,mn}^1(0)^T\quad \mathbf{0}\quad \mathbf{0}\quad \mathbf{0}\quad \mathbf{0}\quad \mathbf{0}]^T\,,$$

$$\mathbf{M}_{mn}^p=[\mathbf{0}\quad \mathbf{0}\quad \mathbf{0}\quad \mathbf{0}\quad \mathbf{0}\quad \mathbf{T}_{5,mn}^p(H)^T\quad \mathbf{T}_{6,mn}^p(H)^T\quad \mathbf{T}_{7,mn}^p(H)^T\quad \mathbf{T}_{4,mn}^p(H)^T\quad \mathbf{T}_{5,mn}^p(H)^T]^T\,,$$

$$\mathbf{Q}_{mn}=[0\quad 0\quad 0\quad 0\quad 0\quad q_{mn}\quad 0\quad 0\quad 0\quad 0]^T\,,$$

where the subscript T means the transpose of the matrix, and $\mathbf{0}$ denotes a 10×1 null sub-matrix. By combining Eqs. (18) and (22), a relation between $\mathbf{C}_{mn}^i(t)$ and $\mathbf{\Delta}_{mn}^i(t)$ can be obtained:

$$\mathbf{\Omega}_{mn}\mathbf{\Gamma}_{mn}(t)=\mathbf{G}_{mn}(t)\ ,\ \text{m,n=1,2,3…,} \tag{23}$$

where

$$\mathbf{\Omega}_{mn}=\begin{bmatrix} -\mathbf{\Psi}_{mn}^1(d_1^1) & \mathbf{\Psi}_{mn}^2(d_2^0) & \mathbf{O} & \cdots & \cdots & \cdots & \cdots & \mathbf{O} \\ \mathbf{O} & -\mathbf{\Psi}_{mn}^2(d_2^1) & \mathbf{\Psi}_{mn}^3(d_3^0) & \mathbf{O} & \cdots & \cdots & \cdots & \mathbf{O} \\ \cdots & \cdots & \cdots & \cdots & \cdots & \cdots & \cdots & \cdots \\ \mathbf{O} & \cdots & \mathbf{O} & -\mathbf{\Psi}_{mn}^i(d_i^1) & \mathbf{\Psi}_{mn}^{i+1}(d_{i+1}^0) & \mathbf{O} & \cdots & \mathbf{O} \\ \cdots & \cdots & \cdots & \cdots & \cdots & \cdots & \cdots & \cdots \\ \mathbf{O} & \cdots & \cdots & \cdots & \cdots & \mathbf{O} & -\mathbf{\Psi}_{mn}^{p-1}(d_{p-1}^1) & \mathbf{\Psi}_{mn}^p(d_p^0) \\ \mathbf{M}_{mn}^1 & \mathbf{O} & \cdots & \cdots & \cdots & \cdots & \mathbf{O} & \mathbf{M}_{mn}^p \end{bmatrix}$$

$$,\ \mathbf{\Gamma}_{mn}(t)=\begin{bmatrix}\mathbf{C}_{mn}^1(t)\\ \mathbf{C}_{mn}^2(t)\\ \cdots \\ \mathbf{C}_{mn}^p(t)\end{bmatrix},\ \mathbf{G}_{mn}(t)=\begin{bmatrix}\mathbf{\Delta}_{mn}^1(t)\\ \mathbf{\Delta}_{mn}^2(t)\\ \cdots \\ \mathbf{\Delta}_{mn}^{p-1}(t)\\ \mathbf{Q}_{mn}\end{bmatrix},$$

in which, $\mathbf{O}$ is 10×10 null sub-matrix. By using the Cramer's law of linear algebraic equation system, the time-varying coefficients can be expressed by $\delta_{i,mn}^{(u)}$,

$\delta_{i,mn}^{(v)}$, $\delta_{i,mn}^{(w)}$, $\delta_{i,mn}^{(\phi)}$, $\delta_{i,mn}^{(D)}$ and q_{mn} , as follows

$$\Gamma_{mn}^{\lambda}(t)=\sum_{k=1}^{p-1}[\frac{\left|\mathbf{\Omega}_{mn,\lambda,k}^{(u)}\right|}{\left|\mathbf{\Omega}_{mn}\right|}\delta_{k,mn}^{(u)}(t)+\frac{\left|\mathbf{\Omega}_{mn,\lambda,k}^{(v)}\right|}{\left|\mathbf{\Omega}_{mn}\right|}\delta_{k,mn}^{(v)}(t)+\frac{\left|\mathbf{\Omega}_{mn,\lambda,k}^{(w)}\right|}{\left|\mathbf{\Omega}_{mn}\right|}\delta_{k,mn}^{(w)}(t)+\frac{\left|\mathbf{\Omega}_{mn,\lambda,k}^{(\phi)}\right|}{\left|\mathbf{\Omega}_{mn}\right|}\delta_{k,mn}^{(\phi)}(t)$$

$$+\frac{\left|\mathbf{\Omega}_{mn,\lambda,k}^{(D)}\right|}{\left|\mathbf{\Omega}_{mn}\right|}\delta_{k,mn}^{(D)}(t)]+\frac{\left|\mathbf{\Omega}_{mn,\lambda}^{(q)}\right|}{\left|\mathbf{\Omega}_{mn}\right|}q_{mn}, \text{ m,n=1,2,3…, } \lambda=1,2…10p, \quad (24)$$

where $\Gamma_{mn}^{\lambda}(t)$ is the λ -th element of $\mathbf{\Gamma}_{mn}(t)$; the matrix with double vertical lines, e.g., $\left|\mathbf{\Omega}_{mn}\right|$, represents the determinant of the matrix; $\mathbf{\Omega}_{mn,\lambda,k}^{(u)}$, $\mathbf{\Omega}_{mn,\lambda,k}^{(v)}$, $\mathbf{\Omega}_{mn,\lambda,k}^{(w)}$, $\mathbf{\Omega}_{mn,\lambda,k}^{(\phi)}$, $\mathbf{\Omega}_{mn,\lambda,k}^{(D)}$ and $\mathbf{\Omega}_{mn,\lambda}^{(q)}$ are obtained by replacing the λ -th column of $\mathbf{\Omega}_{mn}$ with the vector $\mathbf{B}_k^{(u)}$, $\mathbf{B}_k^{(v)}$, $\mathbf{B}_k^{(w)}$, $\mathbf{B}_k^{(\phi)}$, $\mathbf{B}_k^{(D)}$ and $\mathbf{B}^{(q)}$, respectively, in which,

$$\mathbf{B}_k^{(u)}=[\underbrace{0 \quad \cdots \quad 0}_{10k-10} \quad 1 \quad \underbrace{0 \quad \cdots \quad 0}_{10(p-k)+9}]^T,$$

$$\mathbf{B}_k^{(v)}=[\underbrace{0 \quad \cdots \quad 0}_{10k-9} \quad 1 \quad \underbrace{0 \quad \cdots \quad 0}_{10(p-k)+8}]^T,$$

$$\mathbf{B}_k^{(w)}=[\underbrace{0 \quad \cdots \quad 0}_{10k-1} \quad 1 \quad \underbrace{0 \quad \cdots \quad 0}_{10(p-k)}]^T,$$

$$\mathbf{B}_k^{(\phi)}=[\underbrace{0 \quad \cdots \quad 0}_{10k-1} \quad 1 \quad \underbrace{0 \quad \cdots \quad 0}_{10(p-k)}]^T,$$

$$\mathbf{B}_k^{(D)}=[\underbrace{0 \quad \cdots \quad 0}_{10k-8} \quad 1 \quad \underbrace{0 \quad \cdots \quad 0}_{10(p-k)+7}]^T,$$

$$\mathbf{B}^{(q)}=[\underbrace{0 \quad \cdots \quad 0}_{10p-5} \quad 1 \quad 0 \quad 0 \quad 0 \quad 0]^T, \text{ k=1,2…p-1.}$$

The coefficients for i-th layer can be expressed by

$c_{j,mn}^{i}(t)=\Gamma_{mn}^{10i-10+j}(t)$, m,n=1,2,3…, i=1,2…p, j=1,2…10, (25)

where $c_{j,mn}^{i}(t)$ is the j-th element of $\mathbf{C}_{mn}^{i}(t)$.

1. Laplace transformation

By substituting Eqs. (8), (11) and (25) into Eq. (19), and then conducting Laplace transformation, a set of equations for $\widehat{\delta}_{k,mn}^{(u)}(s)$, $\widehat{\delta}_{k,mn}^{(v)}(s)$, $\widehat{\delta}_{k,mn}^{(w)}(s)$, $\widehat{\delta}_{k,mn}^{(\phi)}(s)$ and $\widehat{\delta}_{k,mn}^{(D)}(s)$ can be obtained

$$(\mathbf{A}_{mn}+\mathbf{F}\frac{s}{s+1/\theta_G^*})\widehat{\mathbf{P}}_{mn}(s)=\frac{1}{s}\mathbf{D}_{mn}, \quad (26)$$

where

$$\mathbf{A}_{mn}=\begin{bmatrix} \mathbf{A}_{mn}^{11} & \mathbf{A}_{mn}^{12} & \mathbf{A}_{mn}^{13} & \mathbf{A}_{mn}^{14} & \mathbf{A}_{mn}^{15} \\ \mathbf{A}_{mn}^{21} & \mathbf{A}_{mn}^{22} & \mathbf{A}_{mn}^{23} & \mathbf{A}_{mn}^{24} & \mathbf{A}_{mn}^{25} \\ \mathbf{A}_{mn}^{31} & \mathbf{A}_{mn}^{32} & \mathbf{A}_{mn}^{33} & \mathbf{A}_{mn}^{34} & \mathbf{A}_{mn}^{35} \\ \mathbf{A}_{mn}^{41} & \mathbf{A}_{mn}^{42} & \mathbf{A}_{mn}^{43} & \mathbf{A}_{mn}^{44} & \mathbf{A}_{mn}^{45} \\ \mathbf{A}_{mn}^{51} & \mathbf{A}_{mn}^{52} & \mathbf{A}_{mn}^{53} & \mathbf{A}_{mn}^{54} & \mathbf{A}_{mn}^{5} \end{bmatrix}, \mathbf{F}=\begin{bmatrix} \mathbf{I} & \mathbf{O}_1 \\ \mathbf{O}_2 & \mathbf{O}_3 \end{bmatrix},$$

$$\mathbf{D}_{mn}=\begin{bmatrix} \mathbf{D}_{mn}^{1} \\ \mathbf{D}_{mn}^{2} \\ \mathbf{D}_{mn}^{3} \\ \mathbf{D}_{mn}^{4} \\ \mathbf{D}_{mn}^{5} \end{bmatrix},$$

$$\widehat{\mathbf{P}}_{mn}(s)=[\widehat{\delta}_{1,mn}^{(u)}(s) \quad \cdots \quad \widehat{\delta}_{(p-1),mn}^{(u)}(s) \quad \widehat{\delta}_{1,mn}^{(v)}(s) \quad \cdots \quad \widehat{\delta}_{(p-1),mn}^{(v)}(s) \quad \widehat{\delta}_{1,mn}^{(w)}(s) \quad \cdots \quad \widehat{\delta}_{(p-1),mn}^{(w)}(s)$$

$$\widehat{\delta}_{1,mn}^{(\phi)}(s) \quad \cdots \quad \widehat{\delta}_{(p-1),mn}^{(\phi)}(s) \quad \widehat{\delta}_{1,mn}^{(D)}(s) \quad \cdots \quad \widehat{\delta}_{(p-1),mn}^{(D)}(s)]^T,$$

in which, s denotes the Laplace transformation variable; the variable with an over curve means the variable is in Laplace transformation shape; $\mathbf{I}$ is a (3p-3)×(3p-3) unit matrix; $\mathbf{O}_1$, $\mathbf{O}_2$ and $\mathbf{O}_3$ are (3p-3)×(2p-2), (2p-2)×(3p-3) and (2p-2)×(2p-2) null matrices, respectively; the elements in $\mathbf{A}_{mn}$ and $\mathbf{D}_{mn}$ are given in Eq. (A4) in Appendix A. By using the Cramer's law to solve Eq. (26), $\widehat{\delta}_{k,mn}^{(u)}(s)$, $\widehat{\delta}_{k,mn}^{(v)}(s)$, $\widehat{\delta}_{k,mn}^{(w)}(s)$, $\widehat{\delta}_{k,mn}^{(\phi)}(s)$ and $\widehat{\delta}_{k,mn}^{(D)}(s)$ can be written into the fractional expression of s

$$\widehat{P}_{mn}^{j}(s)=\frac{\sum_{k=0}^{3p-3}\omega_k^j s^k}{\sum_{k=0}^{3p-3}\eta_k s^{k+1}}, \text{ m,n=1,2,3…, j=1,2…(5p-5),} \quad (27)$$

where $\widehat{P}_{mn}^{j}(s)$ is the j-th element of $\widehat{\mathbf{P}}_{mn}(s)$, and

$\eta_k=\sum_{i=0}^{k}J_{mn,i}C_{3p-3-i}^{3p-3-k}(1/\theta_G^*)^{3p-3-k}$, 0 ≤ k ≤ 3p-3,

$$\omega_k^j=\begin{cases} \sum_{i=0}^{k}[L_{mn,i}^{j}C_{3p-3-i}^{3p-3-k}(1/\theta_G^*)^{3p-3-k}], 0\le k\le 3p-4, 1\le j\le 3p-3, \\ \sum_{i=0}^{3p-4}L_{mn,i}^{j}, k=3p-3, 1\le j\le 3p-3, \\ \sum_{i=0}^{k}[N_{mn,i}^{j}C_{3p-3-i}^{3p-3-k}(1/\theta_G^*)^{3p-3-k}], 0\le k\le 3p-3, 3p-2\le j\le 5p-5, \end{cases}$$

in which, $C_a^b=\frac{a!}{b!(a-b)!}$; according to the permutation and combination theory, if arbitrary i (0 ≤ i ≤ 3p-3) amount of columns in the first 3p-3 columns of the determinant $\left|\mathbf{A}_{mn}\right|$ are replaced by the same columns of $\mathbf{F}$, there will be C_{3p-3}^{i} kinds of results, and $J_{mn,i}$ is the sum of all the results. An example for $J_{mn,i}$ are given in Appendix B. Let us define that $\left|\mathbf{A}_{mn}^{j}\right|$ is the result that the j-th (1 ≤ j ≤ 5p-5) column of $\left|\mathbf{A}_{mn}\right|$ is replaced by the column vector $\mathbf{D}_{mn}$. If arbitrary i (0 ≤ i ≤ 3p-4) amount of columns in the first 3p-3, except for j-th (1 ≤ j ≤ 3p-3), columns of $\left|\mathbf{A}_{mn}^{j}\right|$ are replaced by the same columns of $\mathbf{F}$, there will be C_{3p-4}^{i} kinds of results, and $L_{mn,i}^{j}$ is the sum of the all results. $N_{mn,i}^{j}$ is the result that the j-th ($3p-2 \le j \le 5p-5$) column of each determinant in $J_{mn,i}$ is replaced by $\mathbf{D}_{mn}$. Examples for $L_{mn,i}^{j}$ and $N_{mn,i}^{j}$ are given in Appendix B. Eq. (27) can be furthermore decomposed as

$$\widehat{\mathbf{P}}_{mn}^{j}(s)=\sum_{i=1}^{3p-2}\frac{r_i^j}{s-s_i}\text{, m,n=1,2,3…, j=1,2…(5p-5),} \quad (28)$$

where s_i is the root of $\sum_{k=0}^{3p-3}\eta_k s^{k+1}=0$ and $r_i^j=\sum_{k=0}^{3p-3}\omega_k^j(s_i)^k \Big/ \sum_{k=0}^{3p-3}(k+1)\eta_k(s_i)^k$.

The inversed Laplace transformation of Eq. (28) is

$$P_{mn}^{j}(s)=\sum_{i=1}^{3p-2} r_i^j e^{-s_i t}\text{, m,n=1,2,3…, j=1,2…(5p-5).} \quad (29)$$

Finally, by substituting Eq. (29) into Eq. (24), and then substituting the results into Eqs. (8) and (10), the solution of the time-varying stress, electric displacement, magnetic induction, elastic displacement, electric and magnetic potential fields for the plate can all be obtained.

It should be pointed out that the present method is also suitable for other boundary conditions. For example, the clamped edge can be equivalent to a simply supported one subject to a horizontally distributed loading which can be further determined by the zero displacement condition at the clamped edge.

III. Layered Magneto-Electro-Elastic Cylindrical Shell

In this section we present a brief review of the results given in [116]. As shown in Figure 2, a layered cylindrical shell is designed with internal radius R_1, external radius R_2, thickness H, angle θ_0 and infinite length, consisting of p MEE layers with each thickness h_i, adhesively bonded by thin viscoelastic interlayers with same thickness Δh . A cylindrical coordinate system O-θrz is established to identify the location in the shell. Let d_0^i and d_1^i represent the distances from the internal and external surfaces of i-th MEE layer to the circle center O, respectively. The shell is simply supported and acted by a radial load $F(\theta)$ at the external surface. We deem the cylindrical shell in the state of generalized plane strain, which means the variables associated with stress, displacement, electric and magnetic fields are constant along z direction.

The present study complies with four assumptions:

(1) The shell deformation is small and within the linearity range.
(2) The adhesive interlayer is far thinner than the MEE layers, i.e. $\Delta h \ll h_i$.
(3) Based on the previous assumption, the interlayer displacement is assumed to be linearly distributed along the radial direction, which means the interlayer strain is constant through radial direction.
(4) The interlayer, made of adhesive, is relatively soft in comparison with the MEE layer; thus, its circumferential normal stress layer is negligible.

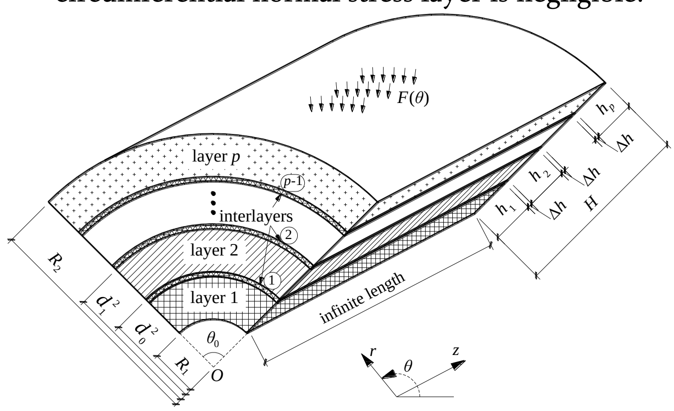

Figure 2. Layered magneto-electro-elastic cylindrical shell with viscoelastic interlayers

Stroh-type general solution for a MEE layer

The coupled constitutive equations for i-th MEE layer can be given in the tensor form

$$\sigma_j^i=c_{jk}^i\gamma_k^i-e_{kj}^iE_k^i-q_{kj}^iH_k^i,$$
$$D_j^i=e_{jk}^i\gamma_k^i+\varepsilon_{jk}^iE_k^i+d_{jk}^iH_k^i,$$
$$B_j^i=q_{jk}^i\gamma_k^i+d_{jk}^iE_k^i+\mu_{jk}^iH_k^i,$$
$$i=1,2\ldots p, \quad (28)$$

where σ_j^i, γ_k^i, D_j^i, E_k^i, B_j^i, H_k^i are the stress, strain, electric displacement, electric field, magnetic induction and magnetic field, respectively; c_{jk}^i, e_{kj}^i, q_{kj}^i, ε_{jk}^i, d_{jk}^i, μ_{jk}^i are elastic, piezoelectric, piezo-magnetic, dielectric, magnetic-permeability and magneto-electric constants, respectively. The general strain-displacement relations in generalized plane stain state are governed by

$$\varepsilon_\theta^i = \frac{u_r^i}{r} + \frac{1}{r}\frac{\partial u_\theta^i}{\partial \theta},\ \varepsilon_r^i = \frac{\partial u_r^i}{\partial r},\ \gamma_{rz}^i = \frac{\partial u_z^i}{\partial r},)$$

$$\gamma_{r\theta}^i = \frac{1}{r}\frac{\partial u_r^i}{\partial \theta} + \frac{\partial u_\theta^i}{\partial r} - \frac{u_\theta^i}{r},\ \gamma_{\theta z}^i = \frac{1}{r}\frac{\partial u_z^i}{\partial \theta},$$

$$E_\theta^i = -\frac{1}{r}\frac{\partial \phi^i}{\partial \theta},\ E_r^i = -\frac{\partial \phi^i}{\partial r},\ H_\theta^i = -\frac{1}{r}\frac{\partial \psi^i}{\partial \theta},$$

$$H_r^i = -\frac{\partial \psi^i}{\partial r},\ \varepsilon_z^i = E_z^i = H_z^i = 0,\ \text{i=1,2…p}, \qquad (29)$$

where u_θ^i, u_z^i, u_r^i are elastic displacement, and ϕ^i and ψ^i are electric and magnetic potentials, respectively. The equilibrium equations, in absence of body forces, electric charge and current density, are given by

$$\frac{\partial \sigma_r^i}{\partial r} + \frac{1}{r}\frac{\partial \tau_{r\theta}^i}{\partial \theta} + \frac{\sigma_r^i - \sigma_\theta^i}{r} = 0,$$

$$\frac{\partial \tau_{r\theta}^i}{\partial r} + \frac{1}{r}\frac{\partial \sigma_\theta^i}{\partial \theta} + \frac{2\tau_{r\theta}^i}{r} = 0,\ \frac{\partial \tau_{rz}^i}{\partial r} + \frac{1}{r}\frac{\partial \tau_{\theta z}^i}{\partial \theta} + \frac{\tau_{rz}^i}{r} = 0,$$

$$\frac{\partial D_r^i}{\partial r} + \frac{1}{r}\frac{\partial D_\theta^i}{\partial \theta} + \frac{D_r^i}{r} = 0,\ \frac{\partial B_r^i}{\partial r} + \frac{1}{r}\frac{\partial B_\theta^i}{\partial \theta} + \frac{B_r^i}{r} = 0,$$

i=1,2…p. (30)

The simply supported boundary condition can be expressed as

$$u_r^i = \phi^i = \psi^i = \sigma_\theta^i = \tau_{\theta z}^i = 0,\ \text{at } \theta=0,\ \theta_0,\ \text{i=1,2…p}, \qquad (31)$$

For this boundary condition, the extended displacements, extended out-of-plane and extended in-plane stresses can be expanded into Fourier series, as follows

$$\begin{bmatrix} u_\theta^i(\theta,r,t) \\ u_z^i(\theta,r,t) \\ u_r^i(\theta,r,t) \\ \phi^i(\theta,r,t) \\ \psi^i(\theta,r,t) \end{bmatrix} = \sum_{m=1}^{\infty} \begin{bmatrix} u_{\theta,m}^i(r,t)\cos(\alpha_m\theta) \\ u_{z,m}^i(r,t)\sin(\alpha_m\theta) \\ u_{r,m}^i(r,t)\sin(\alpha_m\theta) \\ \phi_m^i(r,t)\sin(\alpha_m\theta) \\ \psi_m^i(r,t)\sin(\alpha_m\theta) \end{bmatrix},$$

$$\begin{bmatrix} \tau_{r\theta}^i(\theta,r,t) \\ \tau_{rz}^i(\theta,r,t) \\ \sigma_r^i(\theta,r,t) \\ D_r^i(\theta,r,t) \\ B_r^i(\theta,r,t) \end{bmatrix} = \sum_{m=1}^{\infty} \begin{bmatrix} \tau_{r\theta,m}^i(r,t)\cos(\alpha_m\theta) \\ \tau_{rz,m}^i(r,t)\sin(\alpha_m\theta) \\ \sigma_{r,m}^i(r,t)\sin(\alpha_m\theta) \\ D_{r,m}^i(r,t)\sin(\alpha_m\theta) \\ B_{r,m}^i(r,t)\sin(\alpha_m\theta) \end{bmatrix}, \qquad (32)$$

$$\begin{bmatrix} \sigma_\theta^i(\theta,r,t) \\ \sigma_z^i(\theta,r,t) \\ \tau_{\theta z}^i(\theta,r,t) \\ D_\theta^i(\theta,r,t) \\ D_z^i(\theta,r,t) \\ B_\theta^i(\theta,r,t) \\ B_z^i(\theta,r,t) \end{bmatrix} = \sum_{m=1}^{\infty} \begin{bmatrix} \sigma_{\theta,m}^i(r,t)\sin(\alpha_m\theta) \\ \sigma_{z,m}^i(r,t)\sin(\alpha_m\theta) \\ \tau_{\theta z,m}^i(r,t)\cos(\alpha_m\theta) \\ D_{\theta,m}^i(r,t)\cos(\alpha_m\theta) \\ D_{z,m}^i(r,t)\sin(\alpha_m\theta) \\ B_{\theta,m}^i(r,t)\cos(\alpha_m\theta) \\ B_{z,m}^i(r,t)\sin(\alpha_m\theta) \end{bmatrix},\ \text{i=1,2…p.}$$

where $\alpha_m = m\pi/\theta_0$. In view of the differential in Eqs. (29) and (30), the extended displacements and extended out-of-plane stresses are taken as the following form

$$\mathbf{D}_m^i(r,t) = r^{\lambda_m^i}\mathbf{a}_m^i(t),\ \mathbf{O}_m^i(r,t) = r^{\lambda_m^i - 1}\mathbf{b}_m^i(t),\ \text{i=1,2…p, m=1,2,3…}, \qquad (33)$$

where $\mathbf{a}_m^i(t)$ and $\mathbf{b}_m^i(t)$ are both column vectors containing 5 unknown coefficients associated with the time variable t, and

$$\mathbf{D}_m^i(r,t) = [u_{\theta,m}^i(r,t)\ \ u_{z,m}^i(r,t)\ \ u_{r,m}^i(r,t)\ \ \phi_m^i(r,t)\ \ \psi_m^i(r,t)]^T$$

$$\mathbf{O}_m^i(r,t) = [\tau_{r\theta,m}^i(r,t)\ \ \tau_{rz,m}^i(r,t)\ \ \sigma_{r,m}^i(r,t)\ \ D_{r,m}^i(r,t)\ \ B_{r,m}^i(r,t)]^T.$$

By substituting Eqs. (32) and (33) into Eqs. (28)-(30), two relations with respect to $\mathbf{a}_m^i(t)$ and $\mathbf{b}_m^i(t)$ are obtained

$$\mathbf{b}_m^i(t) = (-\mathbf{R}_{im}^T + \mathbf{T}_i\lambda_m^i)\mathbf{a}_m^i(t),$$

$$[\mathbf{Q}_{im} + (\mathbf{R}_{im} - \mathbf{R}_{im}^T)\lambda_m^i + \mathbf{T}_i(\lambda_m^i)^2]\mathbf{a}_m^i(t) = \mathbf{0},\ \text{i=1,2…p, m=1,2,3…}, \qquad (34)$$

where

$$\mathbf{R}_{im} = \begin{bmatrix} c_{55}^i & 0 & \alpha_m c_{13}^i & \alpha_m e_{31}^i & \alpha_m q_{31}^i \\ 0 & 0 & 0 & 0 & 0 \\ -\alpha_m c_{55}^i & 0 & -c_{13}^i & -e_{31}^i & -q_{31}^i \\ -\alpha_m e_{15}^i & 0 & 0 & 0 & 0 \\ -\alpha_m q_{15}^i & 0 & 0 & 0 & 0 \end{bmatrix},$$

$$\mathbf{T}_i = \begin{bmatrix} c_{55}^i & 0 & 0 & 0 & 0 \\ 0 & c_{44}^i & 0 & 0 & 0 \\ 0 & 0 & c_{33}^i & e_{33}^i & q_{33}^i \\ 0 & 0 & e_{33}^i & -\varepsilon_{33}^i & -d_{33}^i \\ 0 & 0 & q_{33}^i & -d_{33}^i & -\mu_{33}^i \end{bmatrix},$$

$$\mathbf{Q}_{im} = \begin{bmatrix} -(\alpha_m)^2 c_{11}^i - c_{55}^i & 0 & \alpha_m(c_{11}^i + c_{55}^i) & \alpha_m e_{15}^i & \alpha_m q_{15}^i \\ 0 & -(\alpha_m)^2 c_{66}^i & 0 & 0 & 0 \\ \alpha_m(c_{11}^i + c_{55}^i) & 0 & -c_{11}^i - (\alpha_m)^2 c_{55}^i & -(\alpha_m)^2 e_{15}^i & -(\alpha_m)^2 q_{15}^i \\ \alpha_m e_{15}^i & 0 & -(\alpha_m)^2 e_{15}^i & (\alpha_m)^2 \varepsilon_{11}^i & (\alpha_m)^2 d_{11}^i \\ \alpha_m q_{15}^i & 0 & -(\alpha_m)^2 q_{15}^i & (\alpha_m)^2 d_{11}^i & (\alpha_m)^2 \mu_{11}^i \end{bmatrix}$$

The second equation in Eq. (34) can be recast into a standard eigenvalue equation, as follows

$$\mathbf{N}_{im} \begin{bmatrix} \mathbf{a}_m^i(t) \\ \mathbf{b}_m^i(t) \end{bmatrix} = \lambda_m^i \begin{bmatrix} \mathbf{a}_m^i(t) \\ \mathbf{b}_m^i(t) \end{bmatrix}, \text{ i=1,2…p, m=1,2,3…,} \quad (35)$$

where

$$\mathbf{N}_{im} = \begin{bmatrix} \mathbf{T}_i^{-1}\mathbf{R}_{im}^T & \mathbf{T}_i^{-1} \\ -\mathbf{Q}_{im} - \mathbf{R}_{im}\mathbf{T}_i^{-1}\mathbf{R}_{im}^T & -\mathbf{R}_{im}\mathbf{T}_i^{-1} \end{bmatrix}.$$

Further, the general solution for the extended displacements and extended out-of-plane stresses is obtained

$$\begin{bmatrix} \mathbf{D}_m^i(r,t) \\ r\mathbf{O}_m^i(r,t) \end{bmatrix} = \mathbf{E}_m^i r^{\mathbf{B}_m^i} \mathbf{C}_m^i(t), \text{ i=1,2…p, m=1,2,3…,} \quad (36)$$

where $\mathbf{B}_m^i$ is a diagonal matrix including 10 eigenvalues of Eq, (35), $\mathbf{E}_m^i$ is a matrix consisting of 10 corresponding eigenvectors, and $\mathbf{C}_m^i(t)$ is a column vector containing 10 unknown coefficients associated with t. We define

$$\mathbf{\Psi}_m^i(r) = \begin{bmatrix} \mathbf{W}_{im}^1(r) \\ \mathbf{W}_{im}^2(r) \end{bmatrix} = \begin{bmatrix} W_{im}^{1,1}(r) & W_{im}^{1,2}(r) & \cdots & W_{im}^{1,10}(r) \\ W_{im}^{2,1}(r) & W_{im}^{2,2}(r) & \cdots & W_{im}^{2,10}(r) \\ \cdots & \cdots & \cdots & \cdots \\ W_{im}^{10,1}(r) & W_{im}^{10,2}(r) & \cdots & W_{im}^{10,10}(r) \end{bmatrix} = \mathbf{E}_m^i r^{\mathbf{B}_m^i}$$

i=1,2…p, m=1,2,3…, (37)

where $\mathbf{W}_{im}^1(r)$ and $\mathbf{W}_{im}^2(r)$ are both 5×10 sub-matrixes. By reusing Eqs. (28)-(30), the general solution for the extended in-plane stresses can be expressed by

$$\begin{bmatrix} \sigma_{\theta,m}^i \\ \sigma_{z,m}^i \end{bmatrix} = \begin{bmatrix} c_{11}^i \\ c_{12}^i \end{bmatrix} \frac{u_{r,m}^i - \alpha_m u_{\theta,m}^i}{r} + \begin{bmatrix} c_{13}^i & e_{31}^i & q_{31}^i \\ c_{23}^i & e_{32}^i & q_{32}^i \end{bmatrix} (\boldsymbol{\kappa}^i)^{-1} \begin{bmatrix} \sigma_{r,m}^i - c_{13}^i \frac{u_{r,m}^i - \alpha_m u_{\theta,m}^i}{r} \\ D_{r,m}^i - e_{31}^i \frac{u_{r,m}^i - \alpha_m u_{\theta,m}^i}{r} \\ B_{r,m}^i - q_{31}^i \frac{u_{r,m}^i - \alpha_m u_{\theta,m}^i}{r} \end{bmatrix}$$

,

$$D_{\theta,m}^i = \frac{e_{15}^i}{c_{55}^i}\tau_{r\theta,m}^i - \alpha_m\left(\frac{e_{15}^i e_{15}^i}{c_{55}^i} + \varepsilon_{11}^i\right)\frac{\phi_m^i}{r} - \alpha_m\left(\frac{e_{15}^i q_{15}^i}{c_{55}^i} + d_{11}^i\right)\frac{\psi_m^i}{r}$$

,

$$B_{\theta,m}^i = \frac{q_{15}^i}{c_{55}^i}\tau_{r\theta,m}^i - \alpha_m\left(\frac{e_{15}^i q_{15}^i}{c_{55}^i} + d_{11}^i\right)\frac{\phi_m^i}{r} - \alpha_m\left(\frac{q_{15}^i q_{15}^i}{c_{55}^i} + \mu_{11}^i\right)\frac{\psi_m^i}{r}$$

,

$$\tau_{\theta z,m}^i = -\alpha_m c_{66}^i \frac{u_{z,m}^i}{r}, \; D_{z,m}^i = \frac{e_{24}^i}{c_{44}^i}\tau_{rz,m}^i, \; B_{z,m}^i = \frac{q_{24}^i}{c_{44}^i}\tau_{rz,m}^i,$$

i=1,2…p, m=1,2,3…, (38)

where

$$\boldsymbol{\kappa}^i = \begin{bmatrix} c_{33}^i & e_{33}^i & q_{33}^i \\ e_{33}^i & -\varepsilon_{33}^i & -d_{33}^i \\ q_{33}^i & -d_{33}^i & -\mu_{33}^i \end{bmatrix}.$$

Equations of an adhesive interlayer

By employing the SLS model, the shear modulus in the interlayer is given by

$$G^*(t) = G_1^* e^{-t/\theta_G^*} + G_2^*, \quad (39)$$

where the variables with superscript * belong to the interlayer, θ_G^* denotes the relaxation time, G_1^* the relaxation moduli and G_2^* the long-term moduli. These parameters can be measured by the creep test. For simplicity, the Poisson's ratio in the interlayer μ^* is assumed to be time-independent. Therefore, the Young's modulus in the interlayer can be expressed by

$$E^*(t) = 2(1+\mu^*)G^*(t). \quad (40)$$

According to the linear viscoelasticity theory, the constitutive equations for the interlayer are given by

$$\sigma_{r,m}^{*i}(t) = E^*(t)\varepsilon_{r,m}^{*i}(0) + \int_0^t E^{*i}(t-\xi)\frac{\partial \varepsilon_{r,m}^{*i}(\xi)}{\partial \xi}d\xi,$$

$$\tau_{r\theta,m}^{*i}(t) = G^*(t)\gamma_{r\theta,m}^{*i}(0) + \int_0^t G^{*i}(t-\xi)\frac{\partial \gamma_{r\theta,m}^{*i}(\xi)}{\partial \xi}d\xi,$$

$$\tau_{r\theta,m}^{*i}(t) = G^*(t)\gamma_{r\theta,m}^{*i}(0) + \int_0^t G^{*i}(t-\xi)\frac{\partial \gamma_{r\theta,m}^{*i}(\theta,\xi)}{\partial \xi}d\xi$$

, i=1,2…p, m=1,2,3…. (41)

This equation indicates the memory effect of viscoelasticity, i.e., the stress at a time depends on not only the current strain but also the strain history. For briefness, Eq. (41) is then rewritten into the Stieltjes convolution form as follows

$$\sigma^{*i}_{r,m}(t) = 2(1+\mu^*)\varepsilon^{*i}_{r,m}(t) \otimes dG^*(t),$$
$$\tau^{*i}_{r\theta,m}(t) = \gamma^{*i}_{r\theta,m}(t) \otimes dG^*(t), \tag{42}$$
$$\tau^{*i}_{rz,m}(t) = \gamma^{*i}_{rz,m}(t) \otimes dG^*(t), \text{ i=1,2…p, m=1,2,3…},$$

where the symbol $\otimes$ means the convolution operation. The stresses in the interlayer are in balance with those in the adjacent MEE layer, i.e.,

$$\sigma^{*i}_{r,m}(t) = \sigma^{i}_{r,m}(d^i_1, t) = \sigma^{i+1}_{r,m}(d^{i+1}_0, t),$$
$$\tau^{*i}_{r\theta,m}(t) = \tau^{*i}_{r\theta,m}(d^i_1, t) = \tau^{*i+1}_{r\theta,m}(d^{i+1}_0, t),$$
$$\tau^{*i}_{rz,m}(t) = \tau^{*i}_{rz,m}(d^i_1, t) = \tau^{*i+1}_{rz,m}(d^{i+1}_0, t), \text{ i=1,2…p, m=1,2,3….} \tag{43}$$

Recalling the third assumption, the strains in the interlayer can be expressed as

$$\varepsilon^{*i}_{r,m}(t) = \frac{u^{i+1}_{r,m}(d^{i+1}_0, t) - u^i_{r,m}(d^i_1, t)}{\Delta h},$$
$$\gamma^{*i}_{r\theta,m}(t) = \frac{\alpha_m}{d^i_1} u^i_{r,m}(d^i_1, t) + \frac{u^{i+1}_{\theta,m}(d^{i+1}_0, t) - u^i_{\theta,m}(d^i_1, t)}{\Delta h} - \frac{u^i_{\theta,m}(d^i_1, t)}{d^i_1},$$
$$\gamma^{*i}_{rz,m}(t) = \frac{u^{i+1}_{z,m}(d^{i+1}_0, t) - u^i_{z,m}(d^i_1, t)}{\Delta h}, \text{ i=1,2…p-1, m=1,2,3….} \tag{44}$$

The imperfect electric conditions between adjacent layers are also considered, which can be given by

$$D^{i+1}_{r,m}(d^{i+1}_0, t) - D^i_{r,m}(d^i_1, t) = -\chi_1 (\frac{\alpha_m}{d^i_1})^2 \phi^i_m(d^i_1, t),$$
$$\phi^{i+1}_m(d^{i+1}_0, t) - \phi^i_m(d^i_1, t) = -\chi_2 D^i_{r,m}(d^i_1, t), \text{ i=1,2…p-1, m=1,2,3….} \tag{45}$$

This equation can express three conditions: (i) weakly dielectrically conducting condition, i.e., χ_1 =0, χ_2 >0; (ii) highly dielectrically conducting condition, i.e., χ_1 >0, χ_2 =0; (iii) the unelectroded condition, i.e., χ_1 = χ_2 =0.

Here, the magnetic conditions between layers are assumed to be perfect, i.e.,

$$B^{i+1}_{r,m}(d^{i+1}_0, t) - B^i_{r,m}(d^i_1, t) = 0, \tag{46}$$
$$\psi^{i+1}_m(d^{i+1}_0, t) - \psi^i_m(d^i_1, t) = 0, \text{ i=1,2…p-1, m=1,2,3….}$$

Solution for the layered system

In view of Eq. (32), the applied load is also expanded into Fourier series, as follows

$$F(\theta) = \sum_{m=1}^{\infty} q_m \sin(\alpha_m \theta), \tag{47}$$

where $q_m = \frac{2}{\theta_0}\int_0^{\theta_0} F(\theta)\sin(\alpha_m\theta)d\theta$. The conditions at the internal and external surface of the shell are given by

$$\mathbf{O}^1_m(R_1, t) = [0 \quad 0 \quad 0 \quad 0 \quad 0]^T,$$
$$\mathbf{O}^p_m(R_2, t) = [0 \quad 0 \quad q_m \quad 0 \quad 0]^T, \text{ m=1,2,3….} \tag{48}$$

Meanwhile, the adjacent conditions of Eqs. (43)-(46) can be rearranged into the matrix form:

$$\frac{\mathbf{K}^i_m}{\Delta h}\begin{bmatrix} \mathbf{D}^i_m(d^i_1, t) \\ d^i_1 \mathbf{O}^i_m(d^i_1, t) \end{bmatrix} + \frac{1}{\Delta h}\begin{bmatrix} \mathbf{D}^{i+1}_m(d^{i+1}_0, t) \\ d^{i+1}_0 \mathbf{O}^{i+1}_m(d^{i+1}_0, t) \end{bmatrix} = \mathbf{\Delta}^*_{im}(t),$$
$$\text{i=1,2…p-1, m=1,2,3…,} \tag{49}$$

where

$$\mathbf{K}^i_m = \begin{bmatrix} -1-\frac{\Delta h}{d^i_1} & 0 & \frac{\Delta h \alpha_m}{d^i_1} & 0 & 0 & 0 & 0 & 0 & 0 & 0 \\ 0 & -1 & 0 & 0 & 0 & 0 & 0 & 0 & 0 & 0 \\ 0 & 0 & -1 & 0 & 0 & 0 & 0 & 0 & 0 & 0 \\ 0 & 0 & 0 & -1 & 0 & 0 & 0 & 0 & \frac{\chi_2}{d^i_1} & 0 \\ 0 & 0 & 0 & 0 & -1 & 0 & 0 & 0 & 0 & 0 \\ 0 & 0 & 0 & 0 & 0 & -1 & 0 & 0 & 0 & 0 \\ 0 & 0 & 0 & 0 & 0 & 0 & -1 & 0 & 0 & 0 \\ 0 & 0 & 0 & 0 & 0 & 0 & 0 & -1 & 0 & 0 \\ 0 & 0 & 0 & \frac{\chi_1(\alpha_m)^2}{d^i_1} & 0 & 0 & 0 & 0 & -1 & 0 \\ 0 & 0 & 0 & 0 & 0 & 0 & 0 & 0 & 0 & -1 \end{bmatrix}$$

,

$$\mathbf{\Delta}^i_m(t) = [\gamma^{*i}_{r\theta,m}(t) \quad \gamma^{*i}_{rz,m}(t) \quad \varepsilon^{*i}_{r,m}(t) \quad 0 \quad 0 \quad 0 \quad 0 \quad 0 \quad 0 \quad 0]^T$$

.

By combining the surface conditions as well as the adjacent conditions, a matrix equation for the unknown coefficients are obtained, as follows

$$\mathbf{\Omega}_m \mathbf{X}_m(t) = \mathbf{G}_m, \text{ m=1,2,3…,} \tag{50}$$

where

$$\mathbf{\Omega}_m = \begin{bmatrix} \frac{\mathbf{K}^1_m}{\Delta h}\mathbf{\Psi}^1_m(d^1_1) & \frac{1}{\Delta h}\mathbf{\Psi}^2_m(d^2_0) & \mathbf{0}_1 & \cdots & \cdots \\ \mathbf{0}_1 & \frac{\mathbf{K}^2_m}{\Delta h}\mathbf{\Psi}^2_m(d^2_1) & \frac{1}{\Delta h}\mathbf{\Psi}^3_m(d^3_0) & \mathbf{0}_1 & \cdots \\ & & \cdots & \cdots & \\ \cdots & \mathbf{0}_1 & \frac{\mathbf{K}^i_m}{\Delta h}\mathbf{\Psi}^i_m(d^i_1) & \frac{1}{\Delta h}\mathbf{\Psi}^{i+1}_m(d^{i+1}_0) & \mathbf{0}_1 \\ & & \cdots & \cdots & \\ \cdots & \cdots & \mathbf{0}_1 & \frac{\mathbf{K}^{p-1}_m}{\Delta h}\mathbf{\Psi}^{p-1}_m(d^{p-1}_1) & \frac{1}{\Delta h}\mathbf{\Psi}^p_m(d^p_0) \\ \mathbf{M}^1_m & \mathbf{0}_1 & \cdots & \mathbf{0}_1 & \mathbf{M}^p_m \end{bmatrix},$$

$$\mathbf{M}_m^1 = \frac{1}{R_1}\begin{bmatrix}\mathbf{W}_{1m}^2(R_1)\\ \mathbf{0}_2\end{bmatrix},\ \mathbf{M}_m^p = \frac{1}{R_2}\begin{bmatrix}\mathbf{0}_2\\ \mathbf{W}_{pm}^2(R_2)\end{bmatrix},$$

$$\mathbf{X}_m(t) = \begin{bmatrix}\mathbf{C}_m^1(t)\\ \mathbf{C}_m^2(t)\\ \cdots\\ \mathbf{C}_m^p(t)\end{bmatrix},\ \mathbf{G}_m = \begin{bmatrix}\mathbf{\Delta}_m^1\\ \mathbf{\Delta}_m^2\\ \cdots\\ \mathbf{\Delta}_m^{p-1}\\ \mathbf{Q}_m\end{bmatrix},$$

$$\mathbf{Q}_m = [0\quad 0\quad 0\quad 0\quad 0\quad 0\quad 0\quad q_m\quad 0\quad 0]^T,$$

in which, $\mathbf{0}_1$ is a 10×10 null matrix, and $\mathbf{0}_2$ is a 5×10 null matrix. By virtue of Cramer's law of linear equations, the unknown coefficients can be expressed by the interlayer strains

$$X_m^\beta(t) = \sum_{k=1}^{p-1}[\frac{|\mathbf{\Omega}_{m,\beta,k}^{(\theta)}|}{|\mathbf{\Omega}_m|}\gamma_{r\theta,m}^{*k}(t) + \frac{|\mathbf{\Omega}_{m,\beta,k}^{(z)}|}{|\mathbf{\Omega}_m|}\gamma_{rz,m}^{*k}(t) + \frac{|\mathbf{\Omega}_{m,\beta,k}^{(r)}|}{|\mathbf{\Omega}_m|}\varepsilon_{r,m}^{*k}(t)] + \frac{|\mathbf{\Omega}_{m,\beta}^{(q)}|}{|\mathbf{\Omega}_m|}q_m$$

$$C_{im}^j(t) = X_m^{10i-10+j}(t),$$

i=1,2…p, m=1,2,3…, β=1,2…10p, j=1,2…10, (51)

where X_m^β is the β-th element of $\mathbf{X}_m(t)$; C_{im}^j is the j-th element of $\mathbf{C}_m^i(t)$; $\mathbf{\Omega}_{m,\beta,k}^{(\theta)}$, $\mathbf{\Omega}_{m,\beta,k}^{(z)}$, $\mathbf{\Omega}_{m,\beta,k}^{(r)}$, and $\mathbf{\Omega}_{m,\beta}^{(q)}$ are obtained by replacing the β-th column of $\mathbf{\Omega}_m$ with the vector $\mathbf{B}_k^{(\theta)}$, $\mathbf{B}_k^{(z)}$, $\mathbf{B}_k^{(r)}$ and $\mathbf{B}^{(q)}$, respectively, in which,

$$\mathbf{B}_k^{(\theta)} = [\underbrace{0\ \cdots\ 0}_{10k-10}\ 1\ \underbrace{0\ \cdots\ 0}_{10(p-k)+9}]^T,$$

$$\mathbf{B}_k^{(z)} = [\underbrace{0\ \cdots\ 0}_{10k-9}\ 1\ \underbrace{0\ \cdots\ 0}_{10(p-k)+8}]^T,$$

$$\mathbf{B}_k^{(r)} = [\underbrace{0\ \cdots\ 0}_{10k-8}\ 1\ \underbrace{0\ \cdots\ 0}_{10(p-k)+7}]^T,$$

$$\mathbf{B}^{(q)} = [\underbrace{0\ \cdots\ 0}_{10p-3}\ 1\ 0\ 0]^T.$$

By conducting Laplace transformation to Eqs. (39) and (42), one obtains

$$\widehat{G}^*(s) = \frac{G_1^*}{s+1/\theta_G^*} + \frac{G_2^*}{s},$$

$$\widehat{\tau}_{r\theta,m}^i(d_i^1,s) = \widehat{\gamma}_{r\theta,m}^{*i}(s)s\widehat{G}^*(s),$$

$$\widehat{\tau}_{rz,m}^i(d_i^1,s) = \widehat{\gamma}_{rz,m}^{*i}(s)s\widehat{G}^*(s),$$

$$\widehat{\sigma}_{r,m}^i(d_i^1,s) = 2(1+\mu^*)\widehat{\varepsilon}_r^{*i}(s)s\widehat{G}^*(s),$$ i=1,2…p-1, m=1,2,3…, (52)

where the variable with an over curve represents it is in Laplace transformation shape. By substituting Eq. (51) into Eq. (36) and then substituting the results into Eq. (52), the equations for the interlayer strains are obtained

$$(\mathbf{A}_m + \mathbf{I}\frac{s}{s+1/\theta_G^*})\widehat{\mathbf{P}}_m(s) = \frac{1}{s}\mathbf{H}_m,$$ m=1,2,3…, (53)

where $\mathbf{I}$ is the unit matrix, the details of $\mathbf{A}_m$ and $\mathbf{H}_m$ are given in Eq. (A2) of Appendix A, and

$$\widehat{\mathbf{P}}_m(s) = [\widehat{\gamma}_{r\theta,m}^{*1}(s)\ \cdots\ \widehat{\gamma}_{r\theta,m}^{*(p-1)}(s)\ \ \widehat{\gamma}_{rz}^{*1}(s)\ \cdots\ \widehat{\gamma}_{rz}^{*(p-1)}(s)\ \ \widehat{\varepsilon}_{r,m}^{*1}(s)\ \cdots\ \widehat{\varepsilon}_{r,m}^{*(p-1)}(s)]^T$$

By reusing the Cramer's law of linear equations, the solution of interlayer strains in Laplace transformation shape is obtained

$$\widehat{P}_m^j(s) = \frac{\sum_{k=0}^{3p-3}\omega_{k,m}^j s^k}{\sum_{k=0}^{3p-3}\eta_{k,m}s^{k+1}},\ \widehat{\gamma}_{r\theta,m}^{*i}(s) = \widehat{P}_m^i(s),$$

$$\widehat{\gamma}_{rz,m}^{*i}(s) = \widehat{P}_m^{p-1+i}(s),\ \widehat{\varepsilon}_{r,m}^{*i}(s) = \widehat{P}_m^{2p-2+i}(s),$$

m=1,2,3…, j=1,2…3(p-1), i=1,2…p-1, (54)

where $\widehat{P}_m^j(s)$ is the j-th element of $\widehat{\mathbf{P}}_m(s)$, and

$$\omega_{k,m}^j = \begin{cases}\sum_{n=0}^{k}[L_{m,n}^j C_{3p-3-n}^{3p-3-k}(1/\theta_G^*)^{3p-3-k}], 0\le k\le 3p-4,\\ \sum_{n=0}^{3p-4}L_{m,n}^j,\ k=3p-3,\end{cases}$$

$$\eta_{k,m} = \sum_{n=0}^{k}J_{m,n}C_{3p-3-n}^{3p-3-k}(1/\theta_G^*)^{3p-3-k},$$

in which, $C_a^b = \frac{a!}{b!(a-b)!}$; according to the permutation and combination theory, if arbitrary n columns in the determinant $|\mathbf{A}_m|$ are replaced by the same columns of $\mathbf{I}$, there will be C_{3p-3}^n kinds of results, and $J_{m,n}$ is the sum of all results. An example for $J_{m,n}$ is given in Appendix B. Let us define that $|\mathbf{A}_m^j|$ is the result that the j-th column of $|\mathbf{A}_m|$ is replaced by the column vector $\mathbf{H}_m$. If arbitrary n columns of $|\mathbf{A}_m^j|$, except for j-th column, are replaced by the same columns of $\mathbf{I}$, there will be C_{3p-4}^n kinds of results, and $L_{m,n}^j$ is the sum of all results. An example for $L_{m,n}^j$ is given in Appendix B. The inversed Laplace transformation of Eq. (54) is

$P_m^j(t)=\sum_{l=1}^{3p-2} r_{l,m}^j e^{-s_{l,m}t}$, $\gamma_{r\theta,m}^{*i}(t)=\widehat{P}_m^i(t)$,

$\gamma_{rz,m}^{*i}(t)=P_m^{p-1+i}(t)$, $\varepsilon_{r,m}^{*i}(t)=P_m^{2p-2+i}(t)$,

m=1,2,3…, j=1,2…3(p-1), i=1,2…p-1, (55)

where $s_{l,m}$ (l=1,2…3p-2) is the root of the function of s: $\sum_{k=0}^{3p-3}\eta_{k,m}s^{k+1}$ =0, and

$$r_{l,m}^j=\frac{\sum_{k=0}^{3p-3}\omega_{k,m}^j(s_{l,m})^k}{\sum_{k=0}^{3p-3}(k+1)\eta_{k,m}(s_{l,m})^k}.$$

By substituting Eq. (55) into Eq. (51), the coefficients $\mathbf{C}_m^i(t)$ are determined. Finally, the solution for each MEE layer is obtained by substituting $\mathbf{C}_m^i(t)$ into Eq. (36).

It should be mentioned that the present method can also be applied to other boundary conditions. For example, the clamped boundary condition can be equivalent to a simply supported one acted by a distributed load at the edge which can be further determined by the zero displacement condition at the clamped edge.

IV. CONCLUSIONS AND FUTURE DEVELOPMENTS

On the basis of the preceding discussion, following conclusions can be drawn. This review presents an overall view on layered structures of piezoelectric materials.

It is recognized that study on piezoelectric materials becomes a hot topic and has become increasingly popular due their widely applications in engineering fields. However, there are still many possible extensions and areas in need of further development in the future. Among those developments one could list the following:

1. Development of efficient Trefftz finite element-boundary element method schemes for complex piezoelectric structures and the related general purpose computer codes with preprocessing and postprocessing capabilities.
2. Applications of piezoelectric composites to MEMS and smart devices and development of the associated design and fabrication approaches.
3. Extension of the Trefftz-finite element method to elastodynamics of piezoelectric structures, dynamics of thin and thick plate bending and fracture mechanics for structures containing piezoelectric sensor and actuators.
4. Development of multiscale framework across from continuum to micro- and nano-scales for modeling piezoelectric materials and structures.

V. REFERENCES

[1] J. Curie, P. Curie, Development par compression de l'eletricite polaire dans les cristaux hemiedres a faces inclines, Comptes Rendus Acad. Sci. Paris, 91 (1880) 294.
[2] W. Voigt, General theory of the piezo-and pyroelectric properties of crystals, Abh. Gott, 36(1) (1890).
[3] W. Cady, Piezoelectricity, vols. 1 and 2, Dover Publishers, New York, 1964.
[4] H.F. Tiersten, Linear piezoelectric plate vibrations, Springer, New York, 1969.
[5] V.Z. Parton, B.A. Kudryavtsev, Electromagnetoelasticity: piezoelectrics and electrically conductive solids, Gordon and Breach Science Publishers, New York, 1988.
[6] T. Ikeda, Fundamentals of piezoelectricity, Oxford university press, New York, 1996.
[7] N.N. Rogacheva, The theory of piezoelectric shells and plates, CRC Press, Boca Raton, 1994.
[8] Q.H. Qin, Fracture mechanics of piezoelectric materials, WIT Press, Southampton, 2001.
[9] Q.H. Qin, Green's function and boundary elements of multifield materials, Elsevier, Oxford, 2007.
[10] Q.H. Qin, Advanced mechanics of piezoelectricity, Higher Education Press and Springer, Beijing, 2013.
[11] Q.H. Qin, Mechanics of Cellular Bone Remodeling: Coupled Thermal, Electrical, and Mechanical Field Effects, CRC Press, Taylor & Francis, Boca Raton, 2013.
[12] Q.H. Qin, Q.S. Yang, Macro-micro theory on multifield coupling behaivor of hetereogenous

materials, Higher Education Press and Springer, Beijing, 2008.
[13] S. Diao, Q.H. Qin, J. Dong, On branched interface cracks between two piezoelectric materials, Mechanics research communications, 23(6) (1996) 615-620.
[14] Q.H. Qin, Y.W. Mai, Crack branch in piezoelectric bimaterial system, International Journal of Engineering Science, 38(6) (2000) 673-693.
[15] Q.H. Qin, X. Zhang, Crack deflection at an interface between dissimilar piezoelectric materials, International Journal of Fracture, 102(4) (2000) 355-370.
[16] D. Fu, Z. Hou, Q.H. Qin, L. Xu, Y. Zeng, Influence of Shear Stress on Behaviors of Piezoelectric Voltages in Bone, Journal of Applied Biomechanics, 28(4) (2012) 387-393.
[17] D.H. Fu, Z.D. Hou, Q.H. Qin, Analysis of the waveforms of piezoelectric voltage of bone, Journal of Tianjin University, 39 (2006) 349-353.
[18] D.H. Fu, Z.D. Hou, Q.H. Qin, Influence of a notch on the piezoelectric voltages in bone, Engineering Mechanics, 28(1) (2011) 233-237.
[19] D.H. Fu, Z.D. Hou, Q.H. Qin, C. Lu, On the Influence of Relative Humidity on Piezoelectric Signals in Bone, Journal of Experimental Mechanics, 24(5) (2009) 473-478.
[20] Z. Hou, D. Fu, Q.H. Qin, An exponential law for stretching–relaxation properties of bone piezovoltages, International Journal of Solids and Structures, 48(3) (2011) 603-610.
[21] L. Xu, Z. Hou, D. Fu, Q.-H. Qin, Y. Wang, Stretched exponential relaxation of piezovoltages in wet bovine bone, Journal of the Mechanical Behavior of Biomedical Materials, 41 (2015) 115-123.
[22] X. He, C. Qu, Q.H. Qin, A theoretical model for surface bone remodeling under electromagnetic loads, Archive of Applied Mechanics, 78(3) (2008) 163-175.
[23] Q.H. Qin, Thermoelectroelastic solutions for internal bone remodelling under constant loads, Mechanics of electromagnetic solids, 3 (2003) 73-88.
[24] Q.H. Qin, Multi-field bone remodeling under axial and transverse loads, in: D.R. Boomington (Ed.) New research on biomaterials, Nova Science Publishers, New York, 2007, pp. 49-91.
[25] Q.H. Qin, C. Qu, J. Ye, Thermoelectroelastic solutions for surface bone remodeling under axial and transverse loads, Biomaterials, 26(33) (2005) 6798-6810.
[26] Q.H. Qin, J.Q. Ye, Thermoelectroelastic solutions for internal bone remodeling under axial and transverse loads, International Journal of Solids and Structures, 41(9) (2004) 2447-2460.
[27] C. Qu, X. He, Q.H. Qin, Bone functional remodeling under multi-field loadings, Proceedings of the 5th Australasian Congress on Applied Mechanics, (2007) 627-632.
[28] C. Qu, Q.H. Qin, Bone remodeling under multi-field coupled loading, Zhineng Xitong Xuebao(CAAI Transactions on Intelligent Systems), 2(3) (2007) 52-58.
[29] C. Qu, Q.H. Qin, Y. Kang, A hypothetical mechanism of bone remodeling and modeling under electromagnetic loads, Biomaterials, 27(21) (2006) 4050-4057.
[30] X. He, J.S. Wang, Q.H. Qin, Saint-Venant decay analysis of FGPM laminates and dissimilar piezoelectric laminates, Mechanics of Materials, 39(12) (2007) 1053-1065.
[31] K.Q. Hu, Y.L. Kang, Q.H. Qin, A moving crack in a rectangular magnetoelectroelastic body, Engineering Fracture Mechanics, 74(5) (2007) 751-770.
[32] K.Q. Hu, Q.H. Qin, Y.L. Kang, Anti-plane shear crack in a magnetoelectroelastic layer sandwiched between dissimilar half spaces, Engineering Fracture Mechanics, 74(7) (2007) 1139-1147.
[33] Q.H. Qin, Solving anti-plane problems of piezoelectric materials by the Trefftz finite element approach, Computational Mechanics, 31(6) (2003) 461-468.
[34] H.Y. Liu, Q.H. Qin, Y.W. Mai, Theoretical model of piezoelectric fibre pull-out, International Journal of Solids and Structures, 40(20) (2003) 5511-5519.
[35] Q.H. Qin, J.S. Wang, Y.L. Kang, A theoretical model for electroelastic analysis in piezoelectric fibre push-out test, Archive of Applied Mechanics, 75(8-9) (2006) 527-540.
[36] J.S. Wang, Q.H. Qin, Debonding criterion for the piezoelectric fibre push-out test, Philosophical Magazine Letters, 86(2) (2006) 123-136.

[37] J.S. Wang, Q.H. Qin, Y.L. Kang, Stress and electric field transfer of piezoelectric fibre push-out under electrical and mechanical loading, in: Proc. of 9th International Conference on Inspection, Appraisal, Repairs & Maintenance of Structures, Fuzhou, China, 20-21 October, CI-Premier PTY LTD, ISBN: 981-05-3548-1, 2005, pp. 435-442.

[38] Z. Liu, Z. Hou, Q.H. Qin, Y. Yu, L. Tang, On electromechanical behaviour of frog sartorius muscles, in: Engineering in Medicine and Biology Society, 2005. IEEE-EMBS 2005. 27th Annual International Conference of the, IEEE, 2006, pp. 1252-1255.

[39] Q.H. Qin, Using GSC theory for effective thermal expansion and pyroelectric coefficients of cracked piezoelectric solids, International Journal of Fracture, 82(3) (1996) R41-R46.

[40] Q.H. Qin, Y.W. Mai, S.W. Yu, Effective moduli for thermopiezoelectric materials with microcracks, International Journal of Fracture, 91(4) (1998) 359-371.

[41] Q.H. Qin, S.W. Yu, Effective moduli of piezoelectric material with microcavities, International Journal of Solids and Structures, 35(36) (1998) 5085-5095.

[42] Q.H. Qin, S.W. Yu, Using Mori-Tanaka method for effective moduli of cracked thermopiezoelectric materials, in: ICF 9-Sydney, Australia-1997, 1997.

[43] Q.H. Qin, Thermoelectroelastic Green's function for a piezoelectric plate containing an elliptic hole, Mechanics of Materials, 30(1) (1998) 21-29.

[44] Q.H. Qin, Thermoelectroelastic Green's function for thermal load inside or on the boundary of an elliptic inclusion, Mechanics of Materials, 31(10) (1999) 611-626.

[45] Q.H. Qin, Green's function for thermopiezoelectric plates with holes of various shapes, Archive of Applied Mechanics, 69(6) (1999) 406-418.

[46] Q.H. Qin, Green function and its application for a piezoelectric plate with various openings, Archive of Applied Mechanics, 69(2) (1999) 133-144.

[47] Q.H. Qin, Green's functions of magnetoelectroelastic solids with a half-plane boundary or bimaterial interface, Philosophical Magazine Letters, 84(12) (2004) 771-779.

[48] Q.H. Qin, 2D Green's functions of defective magnetoelectroelastic solids under thermal loading, Engineering Analysis with Boundary Elements, 29(6) (2005) 577-585.

[49] Q.H. Qin, Green's functions of magnetoelectroelastic solids and applications to fracture analysis, in: Proc. of 9th International Conference on Inspection, Appraisal, Repairs & Maintenance of Structures, Fuzhou, China, 20-21 October,2005, CI-Premier PTY LTD, ISBN: 981-05-3548-1, 2005, pp. 93-106.

[50] Q.H. Qin, Y.W. Mai, Thermoelectroelastic Green's function and its application for bimaterial of piezoelectric materials, Archive of Applied Mechanics, 68(6) (1998) 433-444.

[51] Q.H. Qin, General solutions for thermopiezoelectrics with various holes under thermal loading, International Journal of Solids and Structures, 37(39) (2000) 5561-5578.

[52] Q.H. Qin, Y.W. Mai, A new thermoelectroelastic solution for piezoelectric materials with various openings, Acta Mechanica, 138(1) (1999) 97-111.

[53] Q.H. Qin, Y.W. Mai, S.W. Yu, Some problems in plane thermopiezoelectric materials with holes, International Journal of Solids and Structures, 36(3) (1999) 427-439.

[54] Q.H. Qin, A new solution for thermopiezoelectric solid with an insulated elliptic hole, Acta Mechanica Sinica, 14(2) (1998) 157-170.

[55] Q.H. Qin, General solutions for thermopiezoelectric materials with various openings, Encyclopedia of Thermal Stresses, (2014) 1932-1942.

[56] Q.H. Qin, Thermoelectroelastic analysis of cracks in piezoelectric half-plane by BEM, Computational Mechanics, 23(4) (1999) 353-360.

[57] Q.H. Qin, Material properties of piezoelectric composites by BEM and homogenization method, Composite structures, 66(1) (2004) 295-299.

[58] Q.H. Qin, Micromechanics-BE solution for properties of piezoelectric materials with defects, Engineering Analysis with Boundary Elements, 28(7) (2004) 809-814.

[59] Q.H. Qin, Micromechanics-BEM Analysis for Piezoelectric Composites, Tsinghua Science & Technology, 10(1) (2005) 30-34.

[60] Q.H. Qin, Boundary Element Method, in: J.S. Yang (Ed.) Special Topics in the Theory of Piezoelectricity, Springer, Cambridge Massachusetts, 2009, pp. 137-168.
[61] Q.H. Qin, Analysis of Piezoelectric Solids through Boundary Element Method, J Appl Mech Eng, 2(1) (2012) e113.
[62] Q.H. Qin, Y.W. Mai, BEM for crack-hole problems in thermopiezoelectric materials, Engineering Fracture Mechanics, 69(5) (2002) 577-588.
[63] Q.H. Qin, Mode III fracture analysis of piezoelectric materials by Trefftz BEM, Structural Engineering and Mechanics, 20(2) (2005) 225-240.
[64] Q.H. Qin, Thermopiezoelectric interaction of macro-and micro-cracks in piezoelectric medium, Theoretical and Applied Fracture Mechanics, 32(2) (1999) 129-135.
[65] Q.H. Qin, Variational formulations for TFEM of piezoelectricity, International Journal of Solids and Structures, 40(23) (2003) 6335-6346.
[66] Q.H. Qin, Fracture Analysis of Piezoelectric Materials by Boundary and Trefftz Finite Element Methods, WCCM VI in conjunction with APCOM'04, Sept. 5-10, 2004, Beijing, China, (2004).
[67] Q.H. Qin, Trefftz Plane Element of Piezoelectric Plate with p-Extension Capabilities, IUTAM Symposium on Mechanics and Reliability of Actuating Materials, (2006) 144-153.
[68] C. Cao, Q.H. Qin, A. Yu, Hybrid fundamental-solution-based FEM for piezoelectric materials, Computational Mechanics, 50(4) (2012) 397-412.
[69] C. Cao, A. Yu, Q.H. Qin, A new hybrid finite element approach for plane piezoelectricity with defects, Acta Mechanica, 224(1) (2013) 41-61.
[70] H. Wang, Q.H. Qin, Fracture analysis in plane piezoelectric media using hybrid finite element model, in: International Conference of fracture, 2013.
[71] Q.H. Qin, M. Lu, BEM for crack-inclusion problems of plane thermopiezoelectric solids, International Journal for Numerical Methods in Engineering, 48(7) (2000) 1071-1088.
[72] Q.H. Qin, Thermoelectroelastic solution for elliptic inclusions and application to crack–inclusion problems, Applied Mathematical Modelling, 25(1) (2000) 1-23.
[73] Q.H. Qin, Y.W. Mai, Crack growth prediction of an inclined crack in a half-plane thermopiezoelectric solid, Theoretical and Applied Fracture Mechanics, 26(3) (1997) 185-191.
[74] H.Y. Liu, Q.H. Qin, Y.W. Mai, Crack growth in composites with piezoelectric fibers, in: Proc. of the Third Int. Conf. for Mesomechanics, Xi'an, China, June 13-16, Tsinghua Univ. Press, Vol. 1, 2000, pp. 357-366.
[75] Q.H. Qin, Y.W. Mai, Multiple cracks in thermoelectroelastic bimaterials, Theoretical and Applied Fracture Mechanics, 29(2) (1998) 141-150.
[76] Q.H. Qin, Y.W. Mai, Thermal analysis for cracks near interfaces between piezoelectric materials, Localized Damage 1998: Fifth International Conference on Damage and Fracture Mechanics, (1998) 13-22.
[77] Q.H. Qin, S.W. Yu, An arbitrarily-oriented plane crack terminating at the interface between dissimilar piezoelectric materials, International Journal of Solids and Structures, 34(5) (1997) 581-590.
[78] Q.H. Qin, S.W. Yu, On the plane piezoelectric problem of a loaded crack terminating at a material interface, Acta Mechanica Solida Sinica, 9 (1996) 151-158.
[79] Q.H. Qin, Y.W. Mai, A closed crack tip model for interface cracks in thermopiezoelectric materials, International Journal of Solids and Structures, 36(16) (1999) 2463-2479.
[80] Q.H. Qin, Y.W. Mai, Crack path selection in piezoelectric bimaterials, Composite structures, 47(1) (1999) 519-524.
[81] Q.H. Qin, J.S. Wang, X. Li, Effect of elastic coating on fracture behaviour of piezoelectric fibre with a penny-shaped crack, Composite structures, 75(1) (2006) 465-471.
[82] J.S. Wang, Q.H. Qin, Penny-shaped Crack in a Solid Piezoelectric Cylinder With Two Typical Boundary Conditions, Journal of Beijing University of Technology, 32(S1) (2006) 29-34.
[83] Q.H. Qin, S. Yu, Logarithmic singularity at crack tips in piezoelectric media, Chinese science bulletin, 41(7) (1996) 563-566.

[84] W. Qiu, Y. Kang, Q. Sun, Q.H. Qin, Y. Lin, Stress analysis and geometrical configuration selection for multilayer piezoelectric displacement actuator, Acta Mechanica Solida Sinica, 17(4) (2004) 323-329.

[85] W. Qiu, Y.L. Kang, Q.H. Qin, Q. Sun, F. Xu, Study for multilayer piezoelectric composite structure as displacement actuator by Moire interferometry and infrared thermography experiments, Materials Science and Engineering: A, 452 (2007) 228-234.

[86] J.S. Wang, Q.H. Qin, Symplectic model for piezoelectric wedges and its application in analysis of electroelastic singularities, Philosophical Magazine, 87(2) (2007) 225-251.

[87] C.-Y. Lee, Q.H. Qin, G. Walpole, Numerical modeling on electric response of fibre-orientation of composites with piezoelectricity, International Journal of Research and Reviews in Applied Science, 16(3) (2013) 377-386.

[88] Q.S. Yang, Q.H. Qin, T. Liu, Interlayer stress in laminate beam of piezoelectric and elastic materials, Composite structures, 75(1) (2006) 587-592.

[89] Q.S. Yang, Q.H. Qin, L. Ma, X. Lu, C. Cui, A theoretical model and finite element formulation for coupled thermo-electro-chemo-mechanical media, Mechanics of Materials, 42(2) (2010) 148-156.

[90] S.W. Yu, Q.H. Qin, Damage analysis of thermopiezoelectric properties: Part I—crack tip singularities, Theoretical and Applied Fracture Mechanics, 25(3) (1996) 263-277.

[91] S.W. Yu, Q.H. Qin, Damage analysis of thermopiezoelectric properties: Part II. Effective crack model, Theoretical and Applied Fracture Mechanics, 25(3) (1996) 279-288.

[92] P. Wu, J. Dong, L. Zhang, Q.-H. Qin, Benchmark solution for multilayer magneto-electro-elastic plates adhesively bonded by viscoelastic interlayer, Journal of Intelligent Material Systems and Structures, 30(3) (2019) 445-462.

[93] H. Wang, Q.H. Qin, Fundamental-solution-based hybrid FEM for plane elasticity with special elements, Computational Mechanics, 48(5) (2011) 515-528.

[94] H. Wang, Q.H. Qin, Fundamental-solution-based finite element model for plane orthotropic elastic bodies, European Journal of Mechanics-A/Solids, 29(5) (2010) 801-809.

[95] M. Dhanasekar, J. Han, Q.H. Qin, A hybrid-Trefftz element containing an elliptic hole, Finite Elements in Analysis and Design, 42(14) (2006) 1314-1323.

[96] Q.H. Qin, C.X. Mao, Coupled torsional-flexural vibration of shaft systems in mechanical engineering—I. Finite element model, Computers & Structures, 58(4) (1996) 835-843.

[97] Q.H. Qin, Hybrid Trefftz finite-element approach for plate bending on an elastic foundation, Applied Mathematical Modelling, 18(6) (1994) 334-339.

[98] Q.H. Qin, The Trefftz finite and boundary element method, WIT Press, Southampton, 2000.

[99] Q.H. Qin, Trefftz finite element method and its applications, Applied Mechanics Reviews, 58(5) (2005) 316-337.

[100] Q.H. Qin, Hybrid-Trefftz finite element method for Reissner plates on an elastic foundation, Computer Methods in Applied Mechanics and Engineering, 122(3-4) (1995) 379-392.

[101] H. Wang, Q.H. Qin, Hybrid FEM with fundamental solutions as trial functions for heat conduction simulation, Acta Mechanica Solida Sinica, 22(5) (2009) 487-498.

[102] Q.H. Qin, H. Wang, Matlab and C programming for Trefftz finite element methods, New York: CRC Press, 2008.

[103] J. Jirousek, Q.H. Qin, Application of hybrid-Trefftz element approach to transient heat conduction analysis, Computers & Structures, 58(1) (1996) 195-201.

[104] Q.H. Qin, X.Q. He, Variational principles, FE and MPT for analysis of non-linear impact-contact problems, Computer methods in applied mechanics and engineering, 122(3) (1995) 205-222.

[105] Y. Cui, J. Wang, M. Dhanasekar, Q.H. Qin, Mode III fracture analysis by Trefftz boundary element method, Acta Mechanica Sinica, 23(2) (2007) 173-181.

[106] W.-G. Jiang, R.-Z. Zhong, Q.H. Qin, Y.-G. Tong, Homogenized Finite Element Analysis on Effective Elastoplastic Mechanical Behaviors of Composite with Imperfect Interfaces,

International Journal of Molecular Sciences, 15(12) (2014) 23389-23407.
[107] H.-W. Wang, Q.H. Qin, H. Ji, Y. Sun, Comparison Among Different Modeling Techniques of 3D Micromechanical Modeling of Damage in Unidirectional Composites, Advanced Science Letters, 4(2) (2011) 400-407.
[108] J. Jirousek, A. Wroblewski, Q.H. Qin, X.Q. He, A family of quadrilateral hybrid-Trefftz p-elements for thick plate analysis, Computer Methods in Applied Mechanics and Engineering, 127(1) (1995) 315-344.
[109] H. Wang, Q.H. Qin, A meshless method for generalized linear or nonlinear Poisson-type problems, Engineering Analysis with Boundary Elements, 30(6) (2006) 515-521.
[110] H. Wang, Q.-H. Qin, Numerical Analysis of Enhanced Heat Transfer in the Metal Foam System Filled with Phase Change Materials, International Journal of Engineering and Information Systems, 1(9) (2017) 129-142.
[111] J. Wang, L. Chen, S. Fang, State vector approach to analysis of multilayered magneto-electro-elastic plates, International Journal of Solids and Structures, 40(7) (2003) 1669-1680.
[112] G. Arzoumanidis, K. Liechti, Linear viscoelastic property measurement and its significance for some nonlinear viscoelasticity models, Mechanics of Time-Dependent Materials, 7(3) (2003) 209-250.
[113] J. Kolařík, A. Pegoretti, Proposal of the Boltzmann-like superposition principle for nonlinear tensile creep of thermoplastics, Polymer Testing, 27(5) (2008) 596-606.
[114] J. Souchek, L.Y. Li, Structure of rings of functions with Riemann Stieltjes convolution products, Journal of Mathematical Analysis and Applications, 41(2) (1973) 468-477.
[115] X. Wang, L. Sudak, A piezoelectric screw dislocation interacting with an imperfect piezoelectric bimaterial interface, International journal of solids and structures, 44(10) (2007) 3344-3358.
[116] P. Wu, C. Hu, Q.-H. Qin, Time-dependent behavior of layered magneto-electro-elastic cylindrical shell with viscoelastic interlayer, Composite Structures, 200 (2018) 874-885.

Cite this article as :

Yi Xiao, "Advance in Layered-Structures of Piezoelectricity", International Journal of Scientific Research in Science, Engineering and Technology (IJSRSET), ISSN : 2456-3307, Volume 6 Issue 1, pp. 336-351, January-February 2019. Available at doi : https://doi.org/10.32628/IJSRSET196164
Journal URL : http://ijsrset.com/IJSRSET196164